



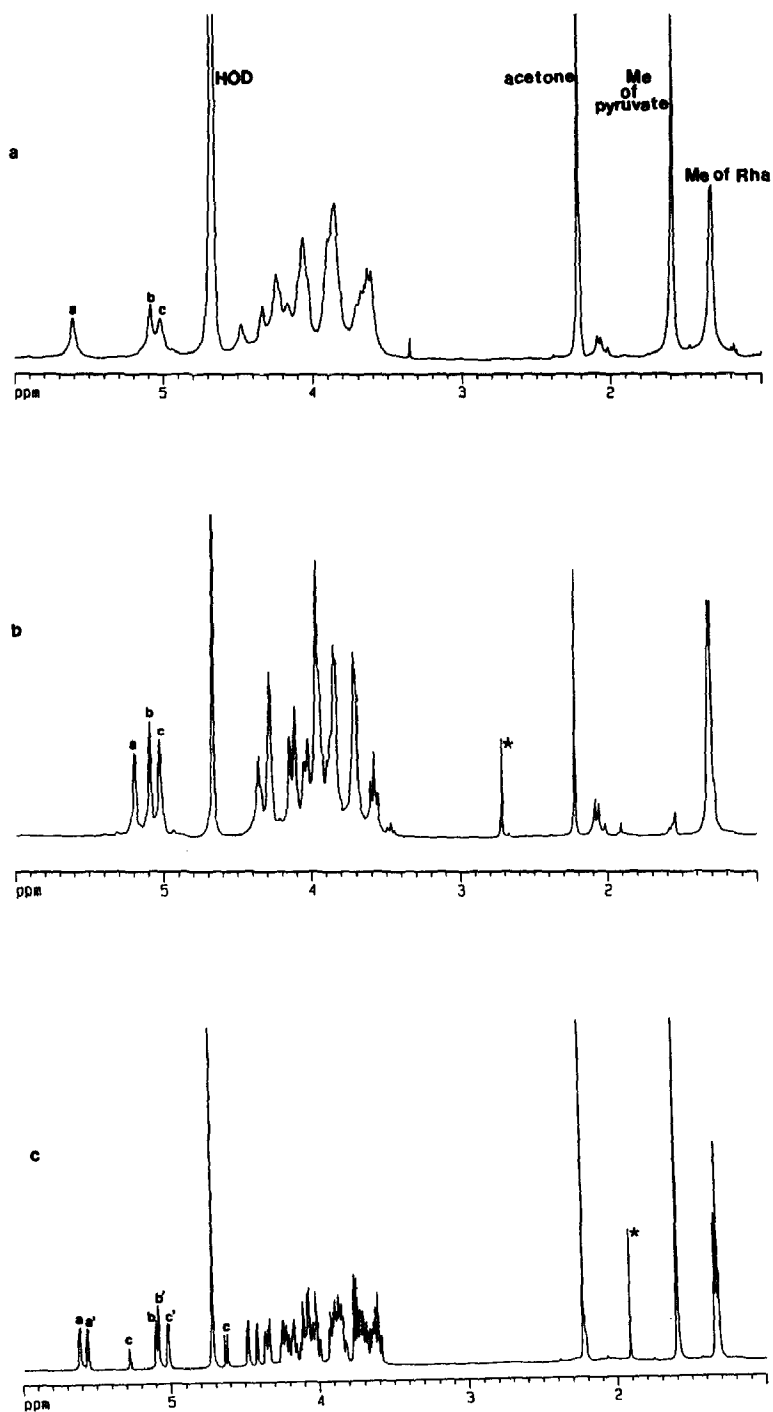
antigen among the Group I polysaccharides [1]. Unlike the other polysaccharides of this group, it has a low molecular weight and is not heat stable. It is, however, acidic and its structure is *Klebsiella*-like, both characteristics of Group I polysaccharides. *E. coli* K103 has been implicated in human appendicitis.

2. Results and discussion

Isolation, composition, and linkage analysis of the capsular antigen.—*E. coli* K103 bacteria were grown on Mueller–Hinton agar and the acidic capsular polysaccharide (PS) was isolated by extraction of the cells using aqueous 1% phenol, and was purified by precipitation with cetyltrimethylammonium bromide. Gel permeation chromatography (GPC) of the PS on Sephacryl S500 showed that it was polydisperse, with the two main fractions having average molecular weights M_r 1.32×10^7 and 3.63×10^4 . Sugar analysis showed the two fractions to be identically constituted. Polydispersity has been reported [2] for other *E. coli* capsular polysaccharides and has been ascribed to the formation of large micellar aggregates by these lipid-bound polysaccharides. When the polysaccharides are treated with dilute acid, the labile phosphodiester bridges linking the polysaccharide chains to lipid are hydrolysed, the micelles are broken down, and much lower molecular weights are observed on GPC (see formation of depyruvated polysaccharide DPS later). Hydrolysis of the PS followed by GLC–MS examination of the derived alditol acetates showed that Gal and Rha were present in the molar ratio 2 : 1. Methanolysis of the PS followed by reduction of the methoxycarbonyl groups, hydrolysis, and GLC examination of the derived alditol acetates showed no alteration of the sugar ratio, indicating the absence of uronic acid. Reaction of the products of methanolysis of the PS with $(CF_3CO)_2O$ followed by GLC analysis on a chiral column [3] established the configuration of both Gal residues as being D and that of Rha as L.

The 1H NMR spectrum of the sodium salt of the PS in D_2O (Fig. 1a) contained H-1 signals at δ 5.61, 5.09, and 5.02, a signal for the methyl protons of pyruvate at δ 1.59, and a signal for H-6 of a deoxy sugar at δ 1.33. The acid sensitivity of the pyruvic substituent, particularly at elevated temperatures, precluded the NMR spectroscopic examination of the PS in its acidic form. Interpretation of the NMR spectra of the sodium form of the PS proved difficult because of a significant degree of line broadening caused by the high viscosity of the sample. The PS was therefore depyruvated by treatment with aq 1% CH_3CO_2H at 100°C for 1 h, followed by purification by GPC on Sephacryl S400. All subsequent analyses and 2D NMR spectroscopic studies were carried out on the depyruvated polysaccharide (DPS) thus obtained. The DPS was found by GPC on Sephacryl S400 to have M_r 2.2×10^4 . The 1H NMR spectrum of the DPS (Fig. 1b) confirmed the presence of three monosaccharides in the repeating unit, one being a 6-deoxy sugar. The ^{13}C NMR spectrum complemented the 1H NMR data with signals for C-1 at 96.67, 101.23, and 102.63 ppm, and a signal for C-6 of a deoxy sugar at 17.60 ppm.

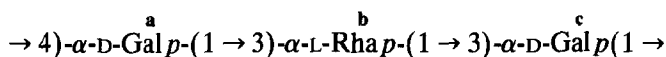
Methylation analysis of the DPS showed the presence of 2,4-di-*O*-methylrhamnose, 2,4,6-tri-*O*-methylgalactose, and 2,3,6-tri-*O*-methylgalactose, indicating that



Figs. 1a–c. ^1H NMR spectra of a, K103 polysaccharide PS; b, depyruvated K103 polysaccharide DPS; c, phage degradation product P2. * Unassigned signals.

the **DPS** contained 3-substituted Rha, 3-substituted Gal, and 4-substituted Gal. **DPS** was incompletely methylated by the Hakomori procedure [4] and the partially methylated polysaccharide was therefore remethylated by the method of Kuhn [5].

2D NMR studies of the E. coli K103 DPS.—The sequence of the residues in the repeating unit was established by 2D NMR experiments, which also confirmed the identity of the constituent residues and the glycosylation sites in the polysaccharide. The residues in the repeating unit were labelled **a–c** in order of decreasing chemical shift of their anomeric protons, as shown in Fig. 1b. The ^1H resonances of all three residues were readily traced via their cross-peaks in the COSY [6] and 2D Homonuclear Hartmann–Hahn (HOHAHA) [7] spectra, while the ^{13}C resonances were assigned by comparing the ^1H assignments with the ^1H – ^{13}C correlation data obtained from an HMQC [8] experiment. These data are shown in Table 1. Comparison of the chemical shift data for residues **a–c** with those reported for methyl glycosides [9,10] permitted identification of residue **a** as 4-substituted Gal, residue **b** as 3-substituted Rha, and residue **c** as 3-substituted Gal. The sequence of the residues in the repeating unit was established by an HMBC [11] experiment. Correlations between H-1 of **a** and C-3 of **b**, between H-1 of **b** and C-3 of **c**, and between H-1 of **c** and C-4 of **a** were clearly visible. The structure of the repeating unit of the **DPS** is thus:



The position of the pyruvic acetal in the repeating unit of the **PS** was established from a study of the hexasaccharide isolated from the bacteriophage depolymerisation of the **PS**.

Bacteriophage-mediated degradation of the PS.—A bacteriophage isolated from sewage water and propagated on the K103 bacteria was used to depolymerise the **PS**. The hexasaccharide (**P2**) obtained, representing two repeating units of the polysaccharide, was purified by GPC on Sephacryl S200 and Bio-Gel P4. The ^1H NMR spectrum of **P2** (Fig. 1c, Table 2) contained five H-1 signals each integrating for one proton, and two fractional H-1 signals in the ratio of 1:3 integrating for

Table 1
NMR data ^a for *E. coli* K103 **DPS**

Residue		Proton or carbon						
		1	2	3	4	5	6a	6b
$\rightarrow 4)\text{-}\alpha\text{-D-Gal}^{\text{a}}$	H	5.20	3.95	4.05	4.15	4.28	3.85	3.85
	C	96.67	69.31	69.89	79.57	71.81	60.98	
$\rightarrow 3)\text{-}\alpha\text{-L-Rha}^{\text{b}}$	H	5.10	4.28	3.96	3.58	3.87	1.32	
	C	102.63	67.71	76.49	71.20	70.03	17.60	
$\rightarrow 3)\text{-}\alpha\text{-D-Gal}^{\text{c}}$	H	5.05	3.97	3.98	4.13	4.36	3.72	3.72
	C	101.23	68.78	77.85	69.70	71.81	61.33	

^a Chemical shifts in ppm with acetone as internal standard, δ 2.23 and 31.07 ppm for ^1H and ^{13}C , respectively.

one proton. These fractional signals at δ 5.25 and 4.63, relating to the α and β forms of the reducing end of **P2**, were further identified as Gal by their $J_{1,2}$ values of 3.1 and 7.4 Hz [9,10]. The anomeric signals were labelled, in order of decreasing chemical shift, as **a**, **a'**, **c _{α}** , **b**, **b'**, **c'**, and **c _{β}** , in order to relate them to the anomeric resonances of the residues already identified in **DPS**. Figs. 1a, 1b, and 1c show the ^1H NMR spectra of the **PS**, the **DPS**, and **P2**, respectively. The H-1 signal for **b** showed slight broadening, as did the H-6 signal for this residue, due to its proximity to the reducing end of the oligosaccharide. A signal for the methyl

Table 2
NMR data ^a for **P2**

Residue		Proton or carbon						
		1	2	3	4	5	6a	6b
a								
→ 4)- α -D-Galp 2,3 V Pyr	H	5.62	4.09	4.24	4.48	4.17	3.86	3.86
	$^3J^b$	3.4		3.6				
	C	94.14	73.49	73.60	75.20	72.77	60.44	
a'								
α -D-Galp 2,3 V Pyr	H	5.56	4.01	4.19	4.42	4.10	3.75	3.75
	$^3J^b$	3.9	9.6	2.6				
	C	93.92	72.73	74.83	67.89	72.33	61.41	
b								
→ 3)- α -L-Rhap	H	5.10	4.36	4.05	3.64	3.89	1.32	
	$^3J^b$	1.8	3.4					
	C	102.57	67.06	75.84	70.80	69.83	17.36	
b'								
→ 3)- α -L-Rhap	H	5.08	4.33	4.03	3.62	3.88	1.33	
	$^3J^b$	1.9	2.6					
	C	102.49	67.03	75.62	70.87	69.83	17.42	
c'								
→ 3)- α -D-Galp	H	5.02	3.91	3.83	4.07	4.24	3.66	3.66
	$^3J^b$	4.0						
	C	100.48	68.45	78.21	69.59	71.44	62.10	
c_{α}								
→ 3)- α -D-GalpOH	H	5.28	3.93	3.90	4.06	4.10	3.70	3.70
	$^3J^b$	3.1						
	C	92.90	68.20	77.89	69.82	71.11	61.65	
c_{β}								
→ 3)- β -D-GalpOH	H	4.63	3.60	3.72	4.02	3.73	3.76	3.76
	$^3J^b$	7.4						
	C	96.89	71.79	81.22	69.14	75.69	61.48	

^a Chemical shifts in ppm with acetone as internal standard, δ 2.23 and 31.07 ppm for ^1H and ^{13}C , respectively.

^b ^1H - ^1H Coupling constants in Hz.

protons of pyruvate occurred at δ 1.59 ($2 \times \text{CH}_3$) and signals for H-6 of the deoxy sugars occurred at δ 1.32 and 1.33, respectively. The ^{13}C spectrum of **P2** contained C-1 signals at 92.90 (fractional), 93.92, 94.14, 96.89 (fractional), 100.48, 102.49, and 102.57 ppm as well as two signals for the pyruvic acetalic carbons at 108.60 and 108.72 ppm. Methyl signals for deoxy sugars occurred at 17.42 and 17.36 ppm, and for pyruvate at 23.17 and 23.37 ppm. Carbonyl signals for pyruvate occurred at 176.45 and 177.18 ppm.

2D NMR studies of P2.—The sequence of the residues in the **P2** unit was established by 2D NMR experiments in the same way as for the **DPS**, using COSY, HOHAHA, DEPT-HMQC [12] (acquired with a read pulse angle of 60° to show CH_2 peaks negative, and CH and CH_3 peaks positive), HETCOR [13], HMQC-TOCSY [14], and HMBC [11] experiments. The COSY spectrum is shown in Fig. 2.

Residues a [$\rightarrow 2,3,4$]- α -D-Gal] and a' [$2,3$]- α -D-Gal].—The ^1H resonances for both of these residues were easily traced via their cross-peaks in the COSY and HOHAHA spectra. The H-4/5 cross-peaks were small, as expected for Gal residues, due to small $J_{4,5}$ values. Carbon resonances were assigned by comparing the ^1H assignments with the ^1H - ^{13}C correlation data obtained from both the HMQC and HETCOR experiments. It was necessary to use both of these correlation experiments because of the amount of signal overlap occurring in various regions of both spectra. The only marked difference in the chemical shift values for the two residues was in those for the C-4 resonance — residue **a** is substituted at this position and the carbon resonance is accordingly at a much lower field than that for residue **a'**.

Residues b and b' [$\rightarrow 3$]- α -L-Rha].—The ^1H and ^{13}C resonances for these two residues were very similar. The ^1H anomeric signal for residue **b** showed slight broadening due to its proximity to the reducing end of **P2**. All ^1H resonances were assigned readily from the COSY spectrum despite the partial overlap from the H-3/4 cross-peak onwards, and the carbon resonances were assigned as for residues **a** and **a'**.

Residues c' and c _{α} [$\rightarrow 3$]- α -D-Gal] and [$\rightarrow 3$]- α -D-GalOH].—The COSY and HOHAHA coupling patterns for these two residues were very similar. ^1H resonances for both residues could be traced as far as H-4 from the cross-peaks in the COSY spectrum, and H-5 and H-6 for **c'** could be identified from the HOHAHA spectrum because a small H-4/5 cross-peak was present. However, no H-4/5 cross-peak was visible for **c _{α}** . Since **c _{α}** is present in smaller quantity than the other residues, the ^1H and ^{13}C peaks for this residue are significantly smaller than those for the other residues. Once all other ^{13}C signals had been assigned, it was possible to identify C-5 and C-6 signals for **c _{α}** from the ^{13}C spectrum, using their comparative heights for confirmation, the corresponding ^1H resonances being assigned from the HETCOR spectrum by correlation. Other ^{13}C resonances were also assigned by correlation using both the HETCOR and HMQC spectra.

Residue c _{β} [$\rightarrow 3$]- β -D-GalOH].—The COSY and HOHAHA coupling patterns for this residue differ markedly from those for residues **a**, **a'**, **c'**, and **c _{α}** because of the β -anomeric configuration. ^1H resonances could be identified as far as H-4 from both the COSY and HOHAHA spectra, and ^{13}C resonances were assigned

from the HMQC and HETCOR data by correlation. The C-5 and C-6 resonances were assigned by difference, permitting the H-5 and H-6 signals to be identified from the ^1H – ^{13}C correlation data. A further distinction between residue c_β and the other Gal residues occurred in the shift position for C-5, which occurs downfield relative to the C-5 signals for the α -Gal residues, as expected [9].

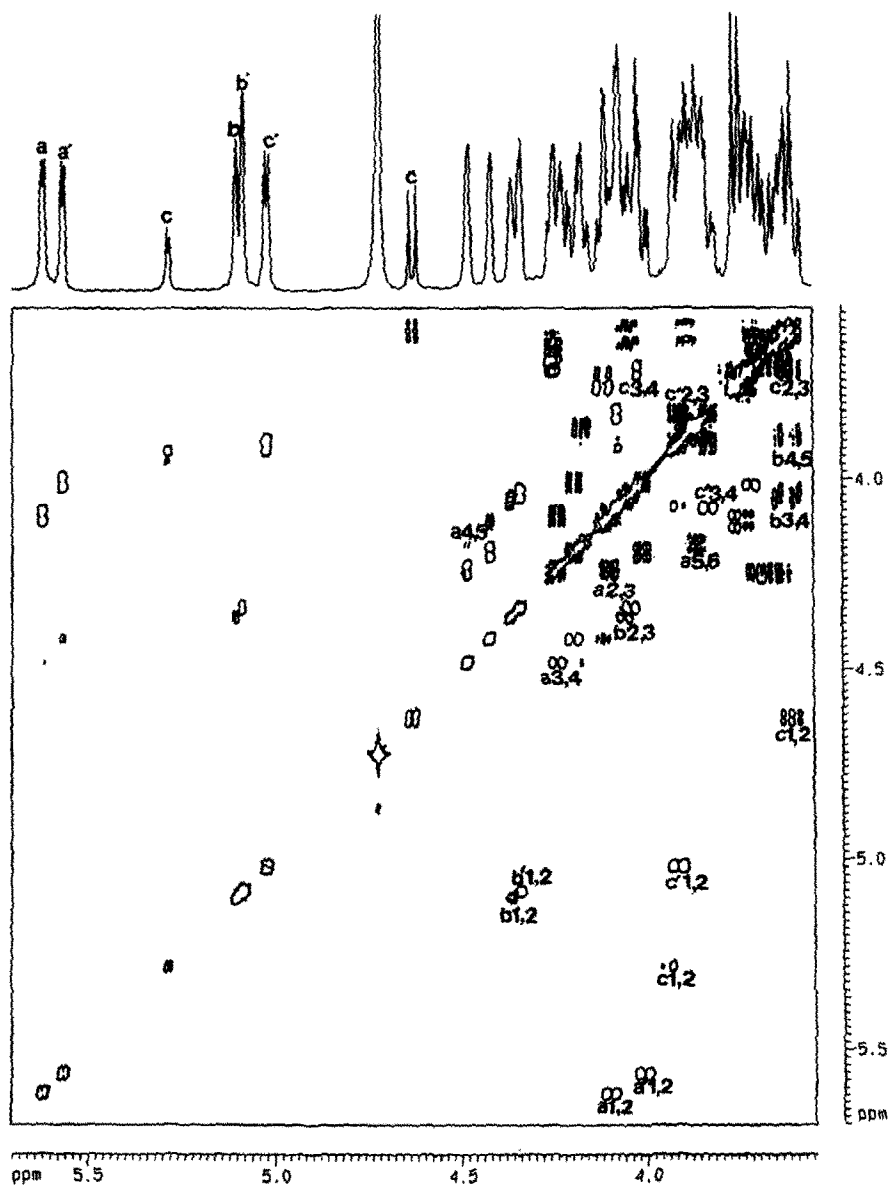


Table 3
Two- and three-bond ^1H – ^{13}C correlations (HMBC) for **P2**

Residue	Proton	Correlation to
a	H-1	75.84 (b , C-3), 73.60 (a , C-3), 72.77 (a , C-5)
	H-2	73.60 (a , C-3)
	H-3	73.49 (a , C-2), 75.20 (a , C-4)
	H-4	100.48 (c' , C-1), 73.49 (a , C-2), 73.60 (a , C-3)
	H-5	75.20 (a , C-4), 60.44 (a , C-6)
a'	H-1	75.62 (b' , C-3), 74.83 (a' , C-3), 72.33 (a' , C-5)
	H-2	74.83 (a' , C-3)
	H-4	72.73 (a' , C-2), 74.83 (a' , C-3)
b	H-1	77.89 (c_α , C-3), 81.22 (c_β , C-3), 67.06 (b , C-2), 75.84 (b , C-3), 69.83 (b , C-5)
	H-2	75.84 (b , C-3), 70.80 (b , C-4)
	H-3	94.14 (a , C-1), 70.80 (b , C-4)
b'	H-1	78.21 (c' , C-3), 67.03 (b' , C-2), 75.62 (b' , C-3), 69.83 (b' , C-5)
	H-3	93.92 (a' , C-1)
c'	H-1	75.20 (a , C-4), 78.21 (c' , C-3), 71.44 (c' , C-5)
	H-2	78.21 (c' , C-3)
	H-3	102.49 (b' , C-1), 69.59 (c' , C-4)
c_α	H-1	77.89 (c_α , C-3), 71.11 (c_α , C-5)
	H-3	102.57 (b , C-1)
c_β	H-1	75.69 (c_β , C-5)
	H-3	102.57 (b , C-1)

The sequence of the residues in **P2** was determined using an HMBC experiment. Clear correlations could be seen between H-1 of **a** and C-3 of **b**, between H-1 of **a'** and C-3 of **b'**, between H-1 of **b** and C-3 of both **c_α** and **c_β**, between H-1 of **b'** and C-3 of **c'**, between H-1 of **c'** and C-4 of **a**, and between C-1 of **c'** and H-4 of **a**, indicating a linkage pattern as shown in the structure below. Other two- and three-bond correlations are listed in Table 3.

The pyruvic acid substituent.—The two 4-substituted Gal residues, **a** and **a'** in **P2**, were shown to be substituted at O-2 and O-3 by the downfield shifts of their C-2 and C-3 resonances as compared to those of residue **a** in the **DPS**. O-2 and O-3 must therefore be the location of the pyruvic substituent in **a** and **a'**. Unfortunately no correlations between the acetalic carbons of the pyruvic substituents and H-2 and H-3 of residues **a** and **a'** were visible in the HMBC spectrum. For this reason, and because the ^1H resonances for the methyl protons of the pyruvic moieties were identical, it was not possible to distinguish between the two pyruvic substituents. The absolute configuration of the acetalic carbon was established from a ROESY [15] experiment performed on **P2**. NOEs were clearly visible between the H-3 signals of both **a** and **a'** and the methyl protons of the pyruvic acetals, indicating that the pyruvic acid had the *S* configuration [16]. The NOEs expected for *R* and *S* configurations, respectively, are shown in Fig. 3.

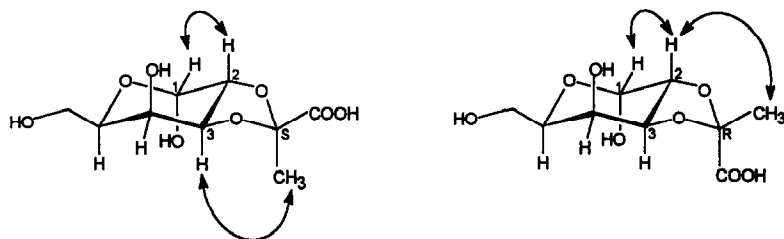


Fig. 3. Expected NOEs for *R* and *S* configurations for a 2,3-linked pyruvic substituent.

Additional NOEs, listed in Table 4, served to confirm the linkages assigned from the HMBC data.

The structure of **P2** can thus be written as:

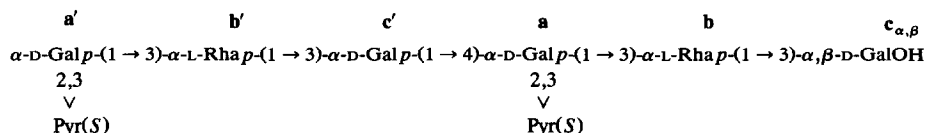


Table 4
NOE data for **P2**

Residue	Proton	NOE to
a	H-1	4.36 (b , H-2), 4.05 (b , H-3), 4.09 (a , H-2), 4.24 (a , H-3)
	H-3	5.62 (a , H-1), 4.48 (a , H-4), 3.86 (a , H-6), 1.59 (pyr)
	H-4	5.02 (c' , H-1), 4.17 (a , H-5), 3.86 (a , H-6)
a'	H-1	4.33 (b' , H-2), 4.03 (b' , H-3), 4.01 (a' , H-2), 4.19 (a' , H-3)
	H-3	5.56 (a' , H-1), 4.42 (a' , H-4), 1.59 (pyr)
	H-4	4.10 (a' , H-5), 3.75 (a' , H-6)
b	H-1	3.93 (c_α , H-2), 3.90 (c_α , H-3), 4.06 (c_α , H-4), 3.60 (c_β , H-2), 3.72 (c_β , H-3), 4.02 (c_β , H-4), 4.36 (b , H-2)
	H-2	5.62 (a , H-1), 5.10 (b , H-1), 4.05 (b , H-3)
	H-6	4.05 (b , H-3), 3.64 (b , H-4), 3.87 (b , H-5)
b'	H-1	3.91 (c' , H-2), 3.83 (c' , H-3), 4.07 (c' , H-4), 4.33 (b' , H-2)
	H-2	5.56 (a' , H-1), 5.08 (b' , H-1), 4.03 (b' , H-3)
	H-6	4.03 (b' , H-3), 3.62 (b' , H-4), 3.87 (b' , H-5)
c'	H-1	4.48 (a , H-4), 3.91 (c' , H-2), 3.83 (c' , H-3)
	H-5	3.83 (c' , H-3), 4.07 (c' , H-4)
c_α	H-1	3.93 (c_α , H-2), 3.90 (c_α , H-3)
	H-4	5.10 (b , H-1), 3.93 (c_α , H-2), 3.90 (c_α , H-3)
c_β	H-1	3.60 (c_β , H-2), 3.73 (c_β , H-3)
	H-4	5.10 (b , H-1), 3.60 (c_β , H-2), 3.72 (c_β , H-3)

and the structure of the repeating unit of the *E. coli* K103 polysaccharide is therefore as shown in the Abstract.

This is the fourth *E. coli* capsular polysaccharide found to contain a pyruvic acid substituent as the sole acidic function [2,17,18]. Although pyruvic acid is a common component of bacterial polysaccharides [19], this is only the second 2,3-linked pyruvic acetal to be reported in the *E. coli* series, the other being found in *E. coli* K33 [20].

3. Experimental

General methods.—Analytical GLC was performed on a Hewlett–Packard 5890A gas chromatograph, fitted with a flame-ionisation detector and a 3392A recording integrator, with He as carrier gas. A J&W Scientific fused-silica DB-17 bonded-phase capillary column (30 m \times 0.25 mm; film thickness, 0.25 μ m) was used for separating alditol acetates (100 kPa, temperature programme: 180°C for 2 min, then 2°C min⁻¹ to 240°C). A J&W Scientific fused-silica DB-225 bonded-phase capillary column (30 m \times 0.25 mm; film thickness, 0.25 μ m) was used for separating partially methylated alditol acetates (100 kPa, 205°C, isothermal). A Machery–Nagel fused-silica FS-Lipodex A capillary column (50 m \times 0.25 mm; film thickness, 0.25 μ m) was used for separating trifluoroacetates of methyl glycosides (150 kPa, temperature programme: 80°C for 1 min, then 2°C min⁻¹ to 150°C). The identities of all derivatives were determined by comparison with authentic standards and confirmed by GLC–MS on a Hewlett–Packard 5988A instrument, using the appropriate column. Spectra were recorded at 70 eV and an ion-source temperature of 200°C. GPC was performed on dextran-calibrated columns (1.6 \times 65 cm) of Sephacryl S500 and Sephacryl S400, using 0.1 M sodium acetate buffer (pH 5.00) as eluent. Compounds were detected by refractive index.

Samples were hydrolysed with 4 M CF₃CO₂H for 1 h at 125°C. Alditol acetates were prepared by reduction of the products in aqueous solutions of hydrolysates with NaBH₄ for 1 h followed by acetylation with 2:1 Ac₂O–pyridine for 1 h at 100°C. Samples were methanolysed by refluxing with methanolic 3% HCl for 16 h. The polysaccharide was depyruvated by treatment with 1% CH₃CO₂H at 100°C for 1 h, followed by dialysis and freeze-drying to give **DPS**. Native and methylated **DPS** samples were carboxyl-reduced with NaBH₄ in dry MeOH after methanolysis. Methylations were carried out on the **DPS** using potassium dimsyl [4] and MeI in Me₂SO, followed by a 48-h Kuhn methylation in DMF with Ag₂O and MeI [5]. For determination of absolute configuration of the constituent monosaccharides, a sample of the **DPS** (10 mg) was methanolysed for 24 h, the product was dissolved in THF (0.5 mL), and two 600- μ L additions of (CF₃CO)₂O were made at 10-min intervals with stirring [21]. The excess of reagent was evaporated and the derived trifluoroacetates were analysed by GLC as described.

Preparation of the K103 polysaccharide.—An authentic culture of *E. coli* O101:K103:H⁻ was obtained from Dr. I. Ørskov (Copenhagen) and propagated on Mueller–Hinton agar. The capsular polysaccharide was extracted with aq 1%

phenol, separated from the cells by ultracentrifugation, and purified by precipitation with cetyltrimethylammonium bromide.

Bacteriophage depolymerisation of K103 polysaccharide.—A bacteriophage that could be propagated on *E. coli* K103 bacteria was isolated from sewage water and was used to depolymerise the capsular polysaccharide. The bacteriophage titre was increased by successive tube and flask lysates [22] until a solution containing 4.0×10^{14} plaque-forming units was obtained. The polysaccharide (300 mg) was dissolved in the bacteriophage solution and incubated at 37°C. After 3 days, the mixture was concentrated and dialysed (mol wt cut-off, 3500) against distilled water (8×50 mL). The combined diffusate was applied first to a column of Sephacryl S200 and eluted with aq 0.1 M sodium acetate buffer (pH 5.00). The main fraction isolated was then applied to a column of Bio-Gel P4 and eluted with water to afford the hexasaccharide **P2** (30 mg).

NMR spectroscopy.—Samples were deuterium-exchanged by freeze-drying several times from D₂O and then examined as solutions in 99.99% D₂O containing a trace of acetone as internal standard (δ 2.23 for ¹H and 31.07 ppm for ¹³C). Spectra were recorded at 30°C on a Bruker AMX-400 spectrometer equipped with an X32 computer. The parameters used for 2D experiments were as follows: COSY and HOHAHA [512 × 2048 data matrix, zero-filled to 1024 data points in t_1 ; 48 or 56 scans per t_1 value; spectral width, 2008 Hz; recycle delay, 1.2 s (COSY) or 1.0 s (HOHAHA); mixing time, 89 ms (HOHAHA); unshifted sine-bell filtering in t_1 and t_2 (COSY); shifted sine-squared filtering in t_1 and t_2 (HOHAHA)]; ROESY [256 × 4096 data matrix, zero-filled to 1024 data points in t_1 ; 104 scans per t_1 value; spectral width, 3846 Hz; recycle delay, 2.0 s; shifted sine-squared filtering in t_1 and t_2 ; carrier frequency placed at far left-hand side of spectrum to minimise COSY and HOHAHA cross-peaks [23]]; DEPT-HMQC and HMQC-TOCSY [256 × 4096 data matrix, zero-filled to 1024 data points in t_1 ; 64 or 76 scans per t_1 value; recycle delay, 1.0 s; fixed delay, 3.45 ms; mixing delay, 89 ms (HMQC-TOCSY); spectral width, 14 086 Hz in t_1 and 2016 Hz in t_2 ; shifted sine-squared filtering in t_1 and t_2 ; read pulse angle, 60°]; HETCOR [128 × 4096 data matrix, zero-filled to 1024 data points in t_1 ; 1500 scans per t_1 value; recycle delay, 1.0 s; fixed delay, 3.45 ms; spectral width, 2200 Hz in t_1 and 10 638 Hz in t_2 ; shifted sine-squared filtering in t_1 and t_2]; HMBC [512 × 4096 data matrix, zero-filled to 1024 data points in t_1 ; 64 scans per t_1 value; recycle delay, 1.0 s; fixed delay, 3.45 ms; spectral width, 20 828 Hz in t_1 and 2024 Hz in t_2 ; shifted sine-squared filtering in t_1 and t_2].

Acknowledgments

We thank Dr. I. Ørskov (Copenhagen) for the test strain of *E. coli* O101:K103:H[−], the Foundation for Research Development (Pretoria) for financial support (to H.P.) and for a doctoral bursary (to M.R.G.), and the Stella and Paul Loewenstein Trust for a doctoral bursary (to M.R.G.).

References

- [1] I. Ørskov, F. Ørskov, B. Jann, and K. Jann, *Bacteriol. Rev.*, 41 (1977) 667–710.
- [2] A.N. Anderson, H. Parolis, and L.A.S. Parolis, *Carbohydr. Res.*, 163 (1987) 81–90, and references therein.
- [3] W.A. König, P. Mischnik-Lübbecke, B. Brassat, S. Lutz, and G. Wenz, *Carbohydr. Res.*, 183 (1988) 11–17.
- [4] L.R. Phillips and B.A. Fraser, *Carbohydr. Res.*, 90 (1981) 149–152.
- [5] R. Kuhn, H. Trischmann, and I. Löw, *Angew. Chem.*, 67 (1955) 32.
- [6] A. Bax and R. Freeman, *J. Magn. Reson.*, 44 (1981) 542–561.
- [7] A. Bax and D.G. Davis, *J. Magn. Reson.*, 65 (1985) 355–360.
- [8] A. Bax and S. Subramanian, *J. Magn. Reson.*, 67 (1986) 565–569.
- [9] J.H. Bradbury and G.A. Jenkins, *Carbohydr. Res.*, 126 (1984) 125–157.
- [10] K. Bock and H. Thørgersen, *Annu. Rep. NMR Spectrosc.*, 13 (1982) 1–57.
- [11] A. Bax and M.F. Summers, *J. Am. Chem. Soc.*, 108 (1986) 2093–2094.
- [12] H. Kessler, P. Schmieder, and M. Kurtz, *J. Magn. Reson.*, 85 (1989) 400–405.
- [13] D.L. Rabenstein and W. Guo, *Anal. Chem.*, 60 (1988) 1R.
- [14] L. Lerner and A. Bax, *J. Magn. Reson.*, 69 (1986) 365–380.
- [15] J. Breg, D. Romun, J.F.G. Vliegthart, G. Strecker, and J. Montreuil, *Carbohydr. Res.*, 183 (1988) 19–34.
- [16] C. Jones, *Carbohydr. Res.*, 198 (1990) 353–357.
- [17] A.H. de Bruin, H. Parolis, and L.A.S. Parolis, *Carbohydr. Res.*, 233 (1992) 195–204.
- [18] M.R. Grue, H. Parolis, and L.A.S. Parolis, 258 (1994) 233–241.
- [19] P.J. Garegg, B. Lindberg, and I. Kvarnström, *Carbohydr. Res.*, 77 (1979) 71–78.
- [20] B.A. Lewis, unpublished results.
- [21] A. Berthold, W.Y. Li, and D. Armstrong, *Carbohydr. Res.*, 201 (1990) 175–184.
- [22] G.G.S. Dutton, J.L. Di Fabio, D.M. Leek, E.H. Merrifield, J.R. Nunn, and A.M. Stephen, *Carbohydr. Res.*, 97 (1981) 127–138.
- [23] A. Bax and D.G. Davis, *J. Magn. Reson.*, 63 (1985) 207–213.